Stainless steel implantation-induced changes in surface characteristics, corrosion resistance and hemato-biochemical parameters of male rat

Sahar A.Fadl-allah[1, 3 *], Q. Mohsen[1] and Nahla S. El-Shenawy[2, 4]

[1]Materials and Corrosion Lab (MCL), Faculty of Science, Taif University, Taif, K.S.A
[2]Zoology Department, Faculty of Science, Taif University, Taif, K.S.A
[3]Chemistry Department, Faculty of Science, Cairo University, Giza, Egypt
[4]Zoology Department, Faculty of Science, Suez Canal University, Ismailia, Egypt
saharfadalla@hotmail.com

Abstract: In this study the physiological solution effect on corrosion resistance and surface characteristics of stainless steel has been studied *in vitro* by electrochemical measurements and microstructure characterization of the surface. All studies were carried out using phosphate buffer saline (PBS) as a simulated physiological solution. Potentiodynamic polarization results indicated a considerable shift of pitting potential of the specimen in the noble direction after14 days of immersion in PBS. As evidenced by electrochemical impedance spectroscopy (EIS), the effect of long immersion of stainless steel in physiological solution on the passive film stability was proved. The surface structure and composition before and after immersion in PBS were then characterized by means of scanning electron microscopy (SEM) with electron diffraction X-ray analysis (EDX) techniques. The electrochemical measurements and fitting parameters showed that the passive film formed on stainless steel decreased the corrosion currents densities (I_{corr}) and the constant phase elements (*CPE*), as simultaneously increased the values of polarization or charge transfer resistance (R_{ct}) of stainless steel in simulated physiological solution. The physiological and histological effects of pitting corrosion of stainless steel metal were studied after 14 days of post-implantation in the tibiae of Sprague-Dawley male rats. The stainless steel implantation caused a slightly increased in blood haemoglobin, total erythrocytes count and packed cell volume, and significantly decreased total leukocyte count. All the hepatic enzymes activities of a separate aminotransferase, alanine aminotransferase, alkaline phosphatase and lactate dehydrogenase were significantly decreased. The activity of glutathione S-transferase and the level of lipid peroxidation were significantly increased while hepatic glutathione was significantly decreased. The toxicity of stainless steel in implanted rat could be related to the biodegradation of the alloy and releasing of Fe, Mn, Ni and Cr in the rat tissue as indicated by the *in vitro* study. The bone regeneration was observed at the surface near the stainless steels implants after two weeks of implantation.

[Sahar A.Fadl-allah, Q. Mohsen and Nahla S. El-Shenawy. **Stainless steel implantation-induced changes in surface characteristics, corrosion resistance and hemato-biochemical parameters of male rat**. Journal of American Science 2011;7(1):84-91]. (ISSN: 1545-1003). http://www.americanscience.org.

***Keywords*:** Impedance spectra; Pitting corrosion; Scanning electron microscope (SEM); Electron diffraction X-ray (EDX) analysis; Lipid peroxidation; Glutathione; Toxicity; Bone repair.

1. Introduction

Biocompatibility is the ability of a material to perform with an appropriate host response in a specific application. This means that the tissue of the patient that comes into contact with the materials does not suffer from any toxic, irritating, inflammatory, allergic, mutagenic, or carcinogenetic action. Hence the attention of researchers to study the corrosion susceptibility of various metals and alloys used in surgical implantation in the physiological fluids (Baroux, 1993). Surgical implants are usually made of metallic materials, such as titanium and its alloys, stainless steels and cobalt - chromium alloys. Among all the metallic materials, stainless steel is the most popular because of their relatively low cost, ease of fabrication and reasonable corrosion resistance. However, stainless steel is susceptible to a number of localized corrosion, such as pitting and crevice corrosion, intergranular corrosion (IGC) and stress corrosion cracking (SCC) (Shaikh et al., 2006). A number of failures of stainless steel materials during its implantation have been reported (Rondelli et al., 2005); due to their high nickel (Ni) content and to the aggressive biological effects. The corrosion products include iron, chromium, nickel and molybdenum. Although new Ni-free stainless steels has been subjected to biological studies and shown promising results (Fini et al., 2003) until now many of the developing countries still use commercial stainless steel which contains Ni element particularly in the filed of bone surgeries. Stainless steel implants are used as temporary implants to help bone healing, as well as fixed implants such as for artificial joints. Typical temporary applications are plates, medullar nails, screws, pins, sutures and steel threads and networks used in fixing fractures (Virtanen et al., 2008). Although stainless steel is seldom used in developed countries as permanent implants, it is still the most used in emerging countries (Ballarre et al., 2010). Stainless steels are iron-base alloys with a minimum of 10.5% Cr as an alloying element, needed to prevent the formation of rust (Haritopoulos et

al., 2007). The susceptibility of stainless steel to the different types of corrosion, especially pitting corrosion depends primarily on the environmental parameters besides the chemical composition and metallurgical manufacturing condition of the steels. The effects of various anions present in surrounding environment on the pitting of stainless steel have been studied by many authors. Zuo et al (2002); reported the inhibition effects of OH^-, NO^{3-}, SO_4^{2-}, ClO_4^- and acetate ions on pitting of stainless steel in chloride solutions. An increase of Cr content strongly increases the resistance against localized breakdown of passivity. Reliable prediction of the corrosion behaviour is the fundamental step towards effective control of corrosion. Electrochemical measurements involving electrochemical polarization and electrochemical impedance spectroscopy techniques were performed in physiological solutions in order to determine and compare the corrosion behaviour of the different implanted materials under variable conditions (Hiromoto et al., 2002). Electrochemical polarization methods are classified as controlled potential (potentiostatic, potentiodynamic) and controlled current (galvanostatic) approaches. The polarization curve associated with a potentiodynamic method allows detailed study of the important parameters that impact the formation and growth of passive films (E_{corr}) and pit propagation (E_{pit}). This method was successfully used to explain the pitting and passivation on stainless steel. On another hand, EIS has been successfully used to investigate the corrosion and passivation phenomena (Fadl-Allah et al., 2008). It enables the direct matching of the electrochemical system to equivalent circuit models. These equivalent circuits consist of discrete electronic components, resistor, capacitors and/or inductors, which can describe the properties of the electrochemical system under investigation.

Despite the high corrosion resistance of stainless steels and good mechanical properties, but corrosion occurs promoting the release of metal ions that penetrate into the biological tissues. The ions that released are disseminated throughout the body and partially accumulated in the liver, kidneys and spleen. Surface characterization of these metallic alloys is highly important as a tool to evaluate the performance of the implant through the interaction surface film-tissue and the possible migration of metallic ions from the base metal to the nearby tissue. The analysis of *in vivo* formation of new tissue at the interfaces of bioactive implants has been reported using histological methods and the interfacial mechanical.

Therefore, the present study was carried out *in vitro* to (1) provide an improved understanding of the corrosion process on stainless steel when soaked in simulated physiological solution which is prepared by dissolving only inorganic components, (2) characterize the relationships between corrosion behaviour and surface characteristics of stainless steel before and after two weeks from its immersion in simulated physiological solution by using scanning electron microscopy (SEM) to study the surface morphology and electron diffraction X-ray analysis (EDX) to analyze the chemical composition of the surface. Moreover, the aim of this study was to evaluate physiological and histological effect of pitting corrosion of local stainless steel metal in osteosynthesis of the body. Some haematological parameters and the alterations in the levels of glutathione, lipid peroxidation and some enzyme activities of liver tissues of male rat were determined after two weeks of post-implantation of commercially stainless steel laminar in tibiae of rat.

2. Materials and methods

2.1 Materials and Chemicals

The implants used in this study were stainless steel with the chemical composition of the metal that is shown as follows: Cr: 19.22%, Ni: 7.8%, Mn: 1.2%, Si: 0.5%, C: 0.019% and Fe: Balance, see Table 1. Samples of stainless steel for electrochemical measurements were machined down to 1 mm in diameter, 3 mm in width and approximately 6 mm in length. They were polished with different grit emery papers up to 4/0 grade, cleaned with distilled water and rinsed in ethanol before mounted in an electrochemical cell. The sample was partially immersed to a constant depth in the testing solution during the experiments. Testing solution of phosphate buffer saline (PBS) [8.77g dm^{-3} sodium chloride (NaCl), 1.42 g dm^{-3} di-sodium hydrogen phosphate (Na_2HPO_4) and 2.72 g dm^{-3} potassium di-hydrogen phosphate (KH_2PO_4)] was prepared from analytical grade reagents and triply distilled water. The test solution was adjusted at pH = 7.4. This test solution was chosen to simulate the physiological solution in order to be able to compare the *in vitro* results with the *in vivo* data.

Table 1. Chemical compositions (in wt%) of the stainless steel samples before (blank) and after immersion in physiological solution (PBS).

Sample	O	Si	Fe	Mn	Ni	Cr	C	Na	P	K	Cl
Blank	-	0.50	68.13	1.22	7.82	19.67	3.11	-	-	-	-
Immersed for 14 days	16.67	-	40.17	0.77	4.34	10.87	7.31	8.19	5.41	1.33	4.94

2.2 *In vitro* experimental and analysis

Electrochemical and Corrosion test

The samples were immersed in simulated solution (PBS) during 14 days. All electrochemical measurements were accomplished with an Autolab (PGSTAT30 with GPES and FRA modules, Ecochemie) in a one compartment three-electrode cell where a platinum wire counter electrode (CE) and a saturated calomel electrode (SCE) as reference to which all potentials are referred. The working electrode (WE) was in the form of a plate cut where the exposed surface areas of the investigated materials was 0.16 cm^2. The potentiodynamic current - potential curves were recorded by changing the electrode potential automatically from – 800 mV to + 2500 mV, just after exposition to the electrolyte solution. The potential scan rate was 1 mV/s. Corrosion current densities (I_{corr}) and corrosion potential (E_{corr}) were evaluated from the intersection of the linear anodic and cathodic branches of the potentiodynamic curve as Tafel plots. Electrochemical impedance spectroscopy (EIS) is a non- destructive sensitive technique which enables the detection of any changes occurring at the electrode/electrolyte interface. Impedance data were presented as Bode plots. Bode plots are recommended as standard impedance plots, since all

impedance data are equally represented and the phase angle, θ, is a sensitive parameter for any surface changes. All EIS spectra were acquired by applying the open circuit potential over a frequency range of 10^{-1}–10^{5} Hz to evaluate the structure stability of stainless steel in PBS. Samples were tested at two periods of immersion time. The results were analyzed using the fit program FRA (Fadl-Allah and Mohsen, 2010). Before impedance or polarization measurements, the working electrodes were immersed in the test solution until a steady state of the open-circuit potential was reached. Each experiment was performed at least twice with a new surface for each run.

Microstructure characterization of surface

Before the polarization experiments, the scanning electron microscope (SEM) photographs were carried out for stainless steel samples to study the morphology of samples before and after immersion in the physiological solution, using SEM Model Philips XL 30 attached with EDX Unit and accelerating voltage 30 kV., magnifications from 1500X up to 15.000X. Samples were coated with a thin layer of gold to prevent charge problem and enhance the resolution. The composition of the surface film, before and after immersion of the samples in physiological solution, was characterized by EDX analysis.

2.3 In *vivo* experiments and analysis
Experimental animals and Implantation

Wistar rats weighing 90-100 g (n = 10) were purchased from King Fahed Medical Research Centre in Jeddah (Kingdom of Saudi Arabia). They were acclimatized and fed *ad libitum* with rodent chow and tap water for a minimum of seven days before surgical process. Animals were randomly divided into two groups with five animals in each; control group and laminar implants group. The European Community Directive (86/609/EEC) and National rules on animal care have been followed. The animals were anesthetized intraperitoneally with a solution of 8 mg ketamine chlorlhydrate and 1.28 mg xylazine per 100 g body weight. The skin of right tibiae was shaved before a 1.5 cm incision was made along the tibial crest. The region of surgery surface was cleaned with antiseptic. The subcutaneous tissue, muscles and ligaments were dissected to expose the lateral external surface of the diaphyseal bone. An end-cutting bur was used to drill a hole 1.5 mm in diameter with manual rotating movements to avoid overheating and necrosis of the bone tissue (Cabrini et al., 1993). No cooling with NaCl was required. No antibiotic therapy was administered. Laminar implants of commercially stainless steel implants of 3.0 × 1.0 × 1.0 mm exhibited a predominantly smooth surface with irregularities that are characteristic of the lamination process. After 14 day of post-implantation, the blood samples were collected from animals in the tube containing ethylenediaminetetraacetic acids (EDTA) under light anaesthesia for blood analysis.

Haematological and Biochemical parameters

Blood samples were collected from the retro-orbital plexus vein of the animals according to Schermer. Blood samples were transferred to test tubes containing EDTA for haematological parameters [red blood cell (RBC) counts, haemoglobin (Hb), packed cells volume (PCV), white blood cell (WBC) counts, lymphocytes counts, mean corpuscular haemoglobin (MCH), mean corpuscular volume (MCV), mean corpuscular haemoglobin concentration (MCHC) and thrombocytes] using Systemax KX21N haematology analyzer. Each sample was run in duplicate.

Liver was removed from rat under ether anaesthesia after 14 day of implantation and washed with cold saline buffer. Washed tissues were immediately stored at -80 ºC. To obtain the enzymatic extract, tissues were homogenized in ice cold 50 mM sodium phosphate buffer (pH 7.0) containing 0.1 mM EDTA to yield 10% (W/V) homogenate. The homogenates were then centrifuged at 4000 rpm for 10 min at 4 ºC. The supernatant were separated and used for determination of enzymes activity of alanine aminotransferase (ALT), a separate aminotransferase (AST), alkaline phosphatase (ALP), lactate dehydrogenase (LDH) and glutathione-S-transferase (GST). The data expressed in international units per gram (IU/g). These biomarkers for liver damage were determined using UV kinetics methodology of the commercial diagnostic kit (Stanbio Co., Spain). Total protein was determined using bovine serum albumin (BSA) as standard and values were expressed as mg/g.
The lipid peroxidation (LPO) was estimated as the concentration of thiobarbituric acid reactive product malondialdehyde (MDA) by using the method of Ohkawa et al. (1979). It was measured spectrophotometrically at 532 nm by using 1,1,3,3-tetraethoxypropane as an external standard. LPO was expressed as MDA in µmol/g of liver tissue. Glutathione (GSH) was measured in tissue homogenates of liver after reaction with 5, 5′-dithiobis-(2-nitrobenzoic acid) using the method of Beutler et al. (1969). The GSH content was expressed as mM GSH/g tissue using a calibration curve prepared by known concentrations of reduced glutathione.

Histopathology

Histopathological examination was carried out according to Drury and Wallington (1980) at the end of the experiment. The animals were killed by ether overdose; the tibiae were removed and fixed in 10% formalin solution for 14–18 h, EDTA solution is used to decalcify bone specimens for histological examination. Then, the samples passed in a series of graded ethanol and embedded in paraffin. Paraffin sections were cut at 5 µm thickness by rotatory microtome and stained with haematoxylin and eosin (H & E) stain for light microscopic examination.

Statistical analysis

Statistical analysis was based on comparing the values between laminar implants group and control group. The results are expressed as means ± SD (n=5). Statistical comparisons were performed using One-way Analysis of Variance (ANOVA) using SPSS statistical software package version 13. The level of significance was taken below $P < 0.05$.

3. Results

3.1 *In vitro* electrochemical measurements

Potentiodynamic polarization

The potentiodynamic polarization technique was used to investigate the electrochemical behaviour of stainless steel in physiological solution, PBS. Representative polarization curves from the potentiodynamic polarization measurements are displayed in Figure. 1. The quantitative corrosion values of corrosion potential (E_{corr}), corrosion current density (I_{corr}), passivation current density (I_{pass}) and pitting potential (E_{pit}) obtained through the polarization curves were calculated and are presented in Table 2. The greatest negative E_{corr} value of -300 mV was observed for the specimen just immersed in PBS. The E_{corr} of specimen was shifted in the noble direction with the time of immersion in PBS. Hysteresis through potential ranging from -300 to 600 mV was found for all stainless steel samples in PBS. These results refer to the passivity is not stable, and indicative of pitting corrosion.

Table 2. Electrochemical parameters calculated from the potentiodynamic polarization curves at different times of immersion of stainless steel samples in physiological solution (PBS).

Immersion time	E_{corr} / mV_{SCE}	E_{pit} / mV_{SCE}	I_{corr} / A cm^{-2}	I_{pass} / A cm^{-2}
Zero time	-300	300	8×10^{-7}	6×10^{-2}
1 day	-20	650	2×10^{-8}	4×10^{-2}
14 days	-250	800	2×10^{-8}	2×10^{-3}

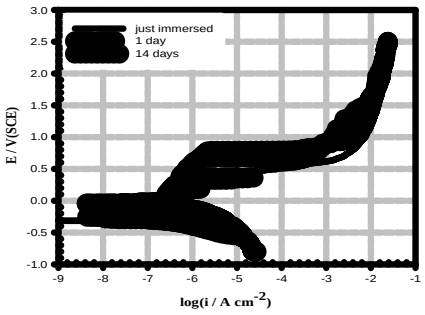

Figure. 1. Polarization curves obtained for Stainless Steel after different times of immersion in phosphate buffer saline (PBS) at pH 7.4.

Impedance measurements

The impedance results for the stainless steel in physiological solution after immersion for two different times are shown in Figure 2. These spectra indicate that the long immersion time of samples in PBS plays an important role to change the properties of the passive film formed on samples. The Bode plots recorded for the stainless steel specimens after zero time (just immersed) and two weeks of immersion in PBS are presented in Figure 2a and 2b respectively. The impedance bode plot (Figure 2a) show that, the impedance resistance of the specimen change with the time of immersion. It is noted that, the impedance values at the minimum frequency range, which correspond to the corrosion resistance of the electrode material, increases with increases the time of specimen immersion in PBS. On the other hand, the phase bode plot (Figure 2b) show that only one phase maximum, which suggests that the time constant of the protective film RC circuit is much greater than that of the double layer RC circuit. This result refer to the corrosion process was mainly charge transfer controlled. The general shape of the curves is similar for all the stainless steel specimens, indicating that almost no change in the corrosion mechanism occurred due to the immersion time (Rosliza et al., 2008). Another parameters related to impedance analysis derived by curve fitting method are summarized in Table 3. Generally, the equivalent circuit model is representing the surface properties of stainless steel specimen in PBS solution and it considers a good way that can be proposed to simulate the experimental results appropriately. Figures 2a and 2b show the computer fitted values and experimental impedance data of specimen in PBS. Charge transfer resistance R_{ct} and capacitance C were obtained by fitting the spectra (0.1-1000Hz) using a simple equivalent mode (Figure 2c). The results showed that R_{ct} values increased with increasing immersion time, the capacitance, C values decrease indicating the formation of a surface film.

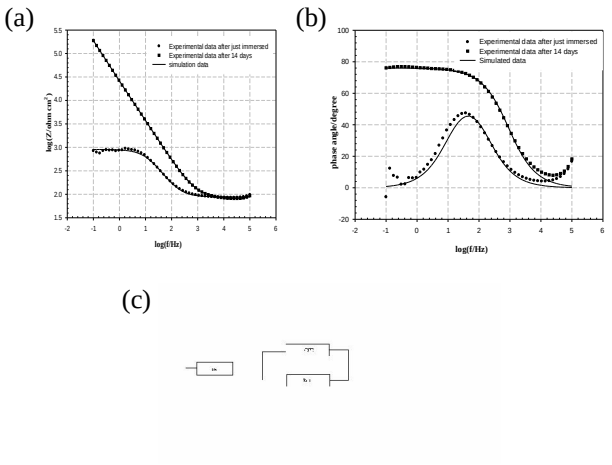

Figure. 2. Impedance data recorded for stainless steel at different immersion times in phosphat buffer saline (PBS) at pH 7.4. (a) Bode-impedance pots, (b) Bode-phase plots, (c) Equivalent circuit used for fitting experimental impedance data where R_s is the solution resistance, R_{ct} is the charge transfer resistance, and CPE is a constant phase elements.

Morphology and composition analysis

Figure 3a presents the SEM of the mechanically polished stainless steel surface. It is observed that the microstructure is characterized by irregularly shaped intermetallic grains with different sizes and their surface distribution is not very homogeneous. This figure indicates that the surface of the specimen is one of the coarse surfaces which increase the biocompatibility of the metal. The grains are separated from

each other by grain boundaries contain small grooves and neither precipitates nor bulk impurities were observed. Figure 3b shows the EDX photographs of the specimen of Figure 3a. Figure 4a shows the SEM of the stainless steel specimen immersed after the aforementioned periods of immersion in PBS. The SEM of Figure 4a shows that the specimen surface after immersion in PBS is covered with a thin slightly homogeneous film. The SEM of high magnification demonstrates the presence of relatively less number of holes between the covered a thin film, Figure 4b. The major observation zoom up more where it was noted the disappearance of the majority of these holes (Figure 4c). Figure 4d shows the EDX photograph of the immersed specimen after 14 days in PBS where there were typical high resolution spectra for Fe and Cr. The concentration of Fe and Cr decreased after exposures as compared to the sample before exposure as indicated in Table 1.

Table 3. Polarization resistance values are calculated by EIS measurements at different time of immersion of stainless steel samples in physiological solution (PBS).

Immersion time	R_s / Ω	R_{ct} / KΩ cm^2	CPE/μF cm^{-2}	n
Zero time	84.51	0.9352	27.74	0.858
14 day	108.29	12491	7.93	0.896

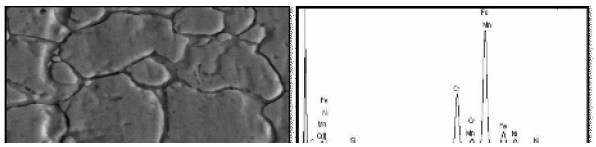

(a) (b)

Figure. 3 (a) Scanning electron micrograph, SEM, and (b) EDX photographs of stainless steel before immersion in phosphate buffer saline (PBS).

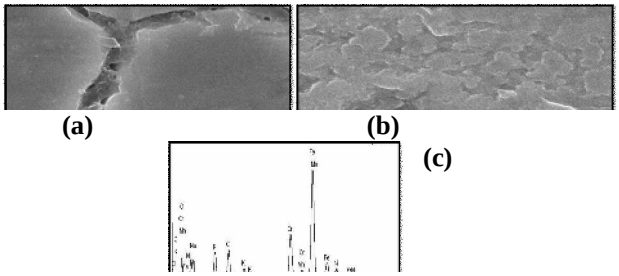

(a) **(b)** **(c)**

Figure 4. (a) Scanning electron micrograph of stainless steel after immersion for 14 days in phosphate buffer saline (PBS) at pH 7.4 with magnification 1500 X, (b) with magnification 10000 X, (c) with magnification 15000 X, and (d) EDX analysis.

3.2 *In vivo* investigation

After implantation of the stainless steel laminar no rat displayed inflammation and there were no unexpected deaths. No weight reduction in any animal was seen during the experimental period. Good healing around the implants was observed without any dehiscence or inflammation.

Table 4. Effect of Stainless Steel implantation for 14 days on haematological parameters of male rat

Parameter	Experimental group	
	Control group	Implanted group
RBCs Parameters		
Hb (g/dl)	9.93 ± 0.47	10.80 ± 0.25
PCV (%)	30.63 ± 3.81	33.33 ± 3.84
TEC (X 10^6)	5.98 ± 0.04	6.15 ± 0.07
RBCs indices		
MCV (fl)	42.40 ± 0.10	42.90 ± 0.01
MCH (pg)	15.60 ± 0.02	17.00 ± 0.12
MCHC (%)	27.20 ± 1.10	25.20 ± 0.34
TLC and DLC %		
TLC (X 10^3)	10.30 ± 0.45	7.00 ± 0.06 [a]
L (%)	69.67 ± 1.20	56.00 ± 0.58 [a]
N (%)	31.67 ± 0.88	44.00 ± 0.58 [a]
Platelets (10^3/mm^3)	667.33 ± 2.73	561.67 ± 13.39 [a]

Hematological and biochemical assay

Hb concentration, PCV% and RBC count slightly increased in the implanted-group. No statistically significant changes were detected in MCH, MCV and MCHC values in implanted-animals as compared to control group at the end of study (Table 4). A significant decrease ($P < 0.01$) in total leukocyte count (TLC) specially percentage of lymphocytes was noticed in implanted-group as compared to the control group, while there was a significant increase ($P < 0.003$) in neutrophils count, reaching to 38.9% of the control value. The significant decrease ($P < 0.05$) in the activities of AST, ALT ALP and LDH (Table 5) after operation could be expected to occur associated with pathology involving necrosis of the liver. As shown in Table 5 the hepatic enzymes LDH and ALP significantly decreased by 2.1-fold and 4.5-fold, respectively, in the implanted-rats as compared to control group indicating plasma membrane damage and liver injury. Antioxidant and oxidative stress of stainless steel corrosion was evaluated by measuring hepatic GST, GSH and LPO (Table 5 and Figure 5) of rat after 14 day of implantation. The present results showed a significant increase in hepatic LPO in stainless steel-implanted rats (Fig. 5). In the present study, decreasing of GSH (Fig. 5) levels in liver tissue under short-term implantation is considered as the primary response to an oxidative-stress-inducing stainless steel.

Values expressed as mean ± SE of 5 separate animals in each group. Blood haemoglobin (Hb), packed cell volume (PCV), total erythrocyte count (TEC), mean corpuscular volume (MCV), mean corpuscular haemoglobin (MCH), mean corpuscular haemoglobin concentration (MCHC), total leukocyte count (TLC), differentiation of leukocytes (DLC), lymphocytes (L), neutrophils (N) and platelets count. [a]Significant different as implanted group compared to control group ($P < 0.001$).

Increasing LPO was associated with the alterations in GST activity (Figure 5 and Table 5). There was an increase in the GST activity at the end of two weeks of stainless steel-implantation ($P < 0.05$) (Table 5).

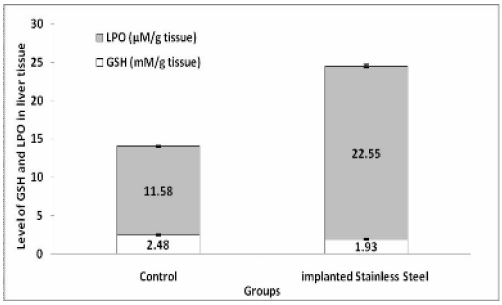

Figure 5. Glutathione (GSH) and lipid peroxidation (LPO) levels of hepatic tissue of male rat after 2 weeks of stainless steel implantation

New bone formation after two weeks of post-implantation as well as a gap between the residual implant and the surrounding bone tissues can be observed in Figure 6A-6D. There are newly formed trabecular and osteoblasts (Figure 6B), indicating that the hole in the tibia gradually healed during degradation of the stainless steel.

Bone tissue histology

The early inflammatory phase comprises the first 2 weeks post injury and is initiated after haemorrhage caused by vascular injury and the subsequent development of a hematoma (Figure 6A and 6B). Infiltration of inflammatory cells and of fibroblasts into the area then occurs (Figure 6A). These events lead to vascularisation of the area and the formation of granulation tissue (that is, procallus) (Figure 6B). The repair phase is characterized by the formation of a callus. It begins with continued vascular in growth, secretion of osteoid, and the presence of fibro collagenous fibers. A temporary callus consisting of cartilage is produced at the site of injury (Figure 6C). Osteoblasts continue to be active and replace cartilage with the cancellous bone forming a bridge between the fractured fragments (Figure 6D).

4. Discussion

4.*1 In vitro* study

The potentiodynamic polarization technique was used to investigate the electrochemical behaviour of stainless steel in PBS. Table 2 shows that the Ecorr for the specimen after 1day of immersion in PBS become more positive than that for the specimen just immersed. This observation suggests that the passive layer is readily formed on stainless steel when it is just immersed in physiological solution. Although, the values of Ecorr for the stainless steel specimen immersed for two weeks is shifted to positive values than that just immersed (Figure.1), it is noted that this Ecorr value is slightly lower than that of stainless specimen immersed for 1day in PBS. This observation probably refers to slightly affected of protection layer with the passage of time for stainless steel specimen in PBS.

As can be seen in Figure 1, it was not possible to evaluate the cathodic Tafel slope as there is no visible linear region that prevents linear extrapolation to E_{corr} of the cathodic polarization curves. This irregularity was confirmed by other researchers and can be explained as the superposition of at least two cathodic current contributions: one arises from oxygen reduction and the second one consequential of metal ion re-deposition (Khaled et al., 2009). It was possible in this case to evaluate, I_{corr}, by extrapolation of the anodic polarization curves only to E_{corr}.

The appearance of hysteresis in the potential region from -300 to 600 mV is evidence that passivity is not stable, and indicative of pitting corrosion. The occurrence of these oscillations was explained by the consecutive formation and repassivation of micro size pits, indicating the formation of so-called metastable pits. The metastable pits are very small in size and grow and repassivate in less than few seconds (Mohammed, 2009). The increase in the current density after hysteresis region is considered an indication of may be complete transition of metastable to stable pitting occurs at E_{pit}. It is noted that the stainless steel immersed for longer time in PBS exhibited more positive E_{pit} values at room temperature than specimens immersed for zero time or short time (Table 2). Although, E_{pitt} is shifted to more positive values when the time of stainless steel immersion increases to two weeks, huge hysteresis is observed. This observation could explain the strong competitive adsorption of cations present in PBS, as Na, K, P, with chloride ions at active surface sits. This explanation was considered as the reason of good corrosion resistance of stainless steel in PBS especially after long period of time in physiological solution (Zuo et al., 2002). The polarization behaviour of all stainless steel specimens in PBS was observed to be almost similar by occurrence of an order of magnitude lower I_{corr} (Table 2). The present study showed that the presence of alloying elements play a significant role in the development of protective film on stainless steel. Generally, this result suggests that this type of stainless steel is quite *in vitro* effective in simulated physiological solution through the formation of a thin protective layer. This explanation is supported by the SEM and EDX analysis.

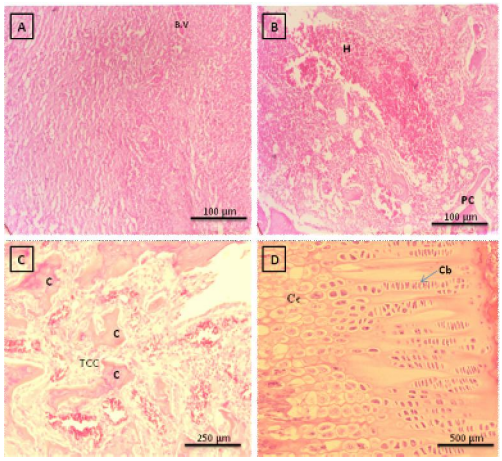

Figure. 6. Photomicrographs H&E stained tissues two weeks after implantation. *A:* Early inflammatory phase of fracture healing is characterized by organizing hematoma. This photomicrograph demonstrates in growth of inflammatory cells, fibroblasts, and small blood vessels (B.V.) into a blood clot, B: The reparative phase consists of fibrosis and woven bone production, characterized by irregular trabeculae of immature bone and osteoid rimmed by osteoblasts, as well as reactive fibro vascular stroma, hematoma (H) and procallaus (PC), C: The late reparative phase is characterized clinically by hard callus formation and temporary cartilage cell, D: Reactive cartilage that is undergoing endochondral ossification; cartilage is growing (expanding) toward the left and cartilage with hypertrophying chondrocytes (Cc) (at left) however, the condroblast (Cb) at right.

The Experimental impedance data were fitted to theoretical data according to different equivalent circuits representing the electrode /electrolyte interface. The best fit was obtained using the simple equivalent circuit presented in Figure 2c. Figure 2a and 2b show the computer fitted values and experimental impedance data of the stainless steel specimens in PBS. This model consists of a parallel combination of a resistor, R_{ct}, representing the charge transfer (corrosion) resistance, and a capacitor, C, representing the electrode capacitance, in series with a resistor, R_s representing the ohmic drop in the electrolyte. However,

better fitting is obtained when constant phase elements (CPE), is used in place of pure capacitance, which it is associated to rough surfaces (Fadl-allah and Mohsen, 2010). The CPE can also include a contribution from dynamic disorder such as diffusion (Al-Mobarak et al., 2006). There is a good agreement between the experimental and theoretical data according to the proposed model. The deviation observed in Figure 2a and 2b can be attributed to the fact that the protective film formed after zero immersion is less homogeneous than that formed after 14 days immersion in PBS.

Impedance parameters derived by curve fitting method are summarized in Table 3. The results showed that R_{ct} values increased with increasing immersion time, the pseudo- capacitive elements present in the circuit are in fact constant phase elements, CPE values decrease indicating the formation of a surface film. The long time of immersion increase the corrosion resistance from 1KΩ to 12491KΩ, but they have of the same order of magnitude (KΩ).The enhancement in corrosion resistance of specimen after long time of immersion can be attributed to formation of passive film can prevent aggressive ions from strong attacking the substrate (Chaves et al., 2006). These findings are consistent with the results obtained by the polarization potentiodynamic tests which observed in Figure 1.Therefore, we can be expect that the formed film after 14 day of specimen immersion in PSB has corrosion resistance up to a good degree but still limited. However, it is also susceptible for the diffusion of chloride ions from PBS through its film/metal interfaces.

It was important to confirm the electrochemical investigations by structural and compositional investigations. Therefore, SEM and EDX measurements were carried out. Many researchers have focused on the imaging the surface of specimen after electrochemical polarization measurements (Elki et al., 2010), but we focused in this study on the imaging metal after enough time of immersion in the simulated physiological solution.

The presence of such a slightly homogeneous film is also confirmed by the EIS characteristics. The observation of morphology and composition analysis supported the results from the potentiodynamic polarization, where we note initiation and passivation of pitting. The presence of these ions (Na, K, P, etc) is confirmed by the EDX investigations, which indicates that the incorporation of the ions from the physiological solution to the protective film and lead to increase its corrosion resistance by time. Moreover, Ni was found after exposure for 14 days with small amount, which suggest that Ni was more completely dissolved from the specimen to the solution during the exposure (Marcus et al., 2008). On the other hand, Cl^- was detected by EDX analysis, which indicates that Cl^- is involved in the surface reaction. This observation supports the results from the polarization and EIS measurements. The penetrations of the chloride ions to the material surface initiate holes which accumulate to form the corrosion spots shown in this scanning electron micrograph.

4.2 *In vivo* study

Enhancement of HB and number of RBCs could be evidence that anemia is not associated with degradation of stainless steel during implantation. Decreasing the TLC could be due to excessive production of wear particles from stainless steel. Rena et al. (2008) reported that TLC plays an important role in engulf particulate debris and becomes activated; releasing proinflammatory cytokines, chemokines, degradative enzymes and reactive oxygen radicals. A significant decrease in platelets count was detected in implanted-group indicated that the rats had thrombocytopenia.

The leakage of intracellular enzymes serves as an index of liver injury, as this enzyme is present in large quantities in the liver (Dufuor et al., 2000; McCuskey and Sipes, 2002). These enzymes escape to the plasma from the injured hepatic cells when cellular degeneration or destruction occurs in this organ (Dufuor et al., 2000). The degradation of the stainless steel as proved *in vitro* study (Table 1) could be the reason to decrease the hepatic enzymes activity after its implantation in rat. The heavy metals in the stainless steel allow derogated by 41.0, 36.88, 44.5 and 44.74% for Fe, Mn, Ni and Cr, respectively after 14 day in PSB. The decrease in the activities of ALP in different tissues might be due to the increased permeability of plasma membrane or cellular necrosis (McCuskey and Sipes, 2002), and this showing the stress condition in implanted-animals.

Decrease in hepatic proteins referred to liver dysfunction as proven by the decrease in liver enzymes activities. The *in vitro* study showed that corrosion products released into the surrounding tissues by stainless 316L orthopaedic implants may affect the expression of the osteogenic phenotype; the *in vivo* mice model, used to investigate the systemic effects induced by the corrosion products *per se*, shed some light on the possible consequences of metal accumulation in organs of vital importance such as the liver, the kidney and the spleen **(**Morals et al., 2000). Mattson (1998) reported that Cr released from implant alloy (polymethylmethacrylate cemented cobalt-chromium) and increased in serum after implantation of the alloy.

Due to high concentration of polyunsaturated fatty acids in cells, LPO is a major outcome of the free radical mediated injury. Two broad outcomes of LPO are structural damage of cellular membranes and generation of oxidized products, some of which are chemically reactive and may covalently modify cellular macromolecules. These reactive products are thought to be the major effecter of tissue damage from LPO (Mattson, 1998). LPO is the additional an indicator of hepatic oxidative injury. This suggests participation of free-radicals induced oxidative cell injury in mediating the toxicity of stainless steel. It was also found that LPO induced by aluminum at sub-lethal levels, alter physiological and biochemical characteristics of biological systems. LPO indicated that there is an unbalance between the productions of oxidants and scavenging of those oxidants by antioxidants (Jaeschke et al., 2002).The result was confirmed by measuring the levels of hepatic GSH. Reduced GSH possesses antioxidant properties and its protective role against oxidative-stress-induced toxicity by keeping reduced of the proteins' –SH groups.

The ability to generate ROS and oxidant injury is one paradigm that may be used to compare the toxic potential of nanoparticles (Xia et al., 2006). Oxidative stress is a state of redox disequilibrium in which ROS production (by the cell or by the nanomaterial itself) overwhelms the antioxidant defense capacity of the cell, thereby leading to adverse biological consequences (Xia et al., 2006): damage of macromolecules, lipids, DNA or proteins resulting in excess cell proliferation, apoptosis, lipid peroxidation, or mutagenesis. The ROS formation by redox reactions may be a critical event in toxic effects if the protective mechanisms of cells are overwhelmed by a strong affinity with nanoparticles. Metallic nanoparticles are known to induce oxidative stress by ROS generation during redox cycling by disruption of the electronic and ionic flux, perturbation of the permeability transition pores and depletion of the cellular glutathione content (Xia et al., 2006).

GST catalyse the addition of the tripeptide glutathione to endogenous and xenobiotics substrates which have electrophilic functional groups. The glutathione adducts produced have increased solubility in water and are subsequently enzymatically degraded to mercapturates and excreted (Hayes et al., 2005). This result confirmed by decreasing the GSH level in implanted-rats which scavenges residual free radicals escaping decomposition by the antioxidant enzymes. GSH plays an excellent role in protecting the cell from LPO.

Oliveira et al. (2004) reported that the effect of metal mixtures (Cu^{2+}+Zn^{2+}, Zn^{2+}+Fe^{2+}, Zn^{2+}+Cr (VI), and Cr (VI)+Fe^{2+}) (100 µM) on liver microsomal EROD activity was assessed, revealing a synergistic interaction. Therefore, the toxicity of stainless steel in implanted rat could be related to the biodegradation of the alloy and

releasing Fe, Mn, Ni and Cr in the rat tissue as indicated *in vitro* study.

There are three main phases following fracture in the bone repair process: 1) the early inflammatory stage; 2) the repair stage; and 3) the remodelling stage. This observations have been described by Hansen-Algenstaedt et al. (2006**)** during the bone repair, These events lead to vascularisation of the area and the formation of granulation tissue (that is, procallus). This initial union has limited strength; thus, internal/external immobilization of the fracture/fusion site is often appropriate. In the remodeling phase the process may occur over months to years and consists of restoring the fractured bone to its normal size, shape, and strength. There was histological evidence of successful bone regeneration, at 2 weeks new bone covered pore space and there was scarce thin fibrous band at the surface near the stainless steels implants.

Acknowledgements

The authors are grateful for the support from the Scientific Research Unit of Taif University. Foundation (No. 1-430-894).

Corresponding author:

Dr. Sahar Ahmed Ali Fadl-Allah

Current address: Materials and Corrosion laboratory, Chemistry Department, Faculty of Science, Taif University, Taif, Saudi Arabia. E-mail address: saharfadalla@hotmail.com

References

1. Baroux B, Passivation and localized corrosion of stainless steel, in: M Forment (Ed.), Passivity of Metals and Semiconductors, Elsevier, Amsterdam,1993;531.
2. Shaikh H, Sivaibharasi N, Sasi B, Anita T, Amirthalingam R, B.P.C. Rao BPC, Jayakumar T, Khatak HS, Baldev Raj. Use of eddy current testing method in detection and evaluation of sensitisation and intergranular corrosion in austenitic stainless steels. Corrosion Science 2006;48(6):1462-1482.
3. Rondelli G, Torricelli P, Fini M, Giardino R. In vitro corrosion study by EIS of a nickel-free stainless steel for orthopaedic applications. Biomaterials 2005;26(7):739-744.
4. Fini M, Nicoli Aldini N,Torricelli P, Giavaresi G, Borsari V, Lenger H, Bernauer J, Giardino R, Chiesa R, Cigada A. A new austenitic stainless steel with negligible nickel content: an in vitro and in vivo comparative investigation. Biomaterials 2003;24(27):4929-4939.
5. Virtanen S, Milošev I, Gomez-Barrena E, Trebše R, Salo J, Konttinen YT. Special modes of corrosion under physiological and simulated physiological conditions. Acta Biomaterialia 2008;4(3);468-476.
6. Ballarre J, Manjubala I, Schreiner WH, Carlos Orellano J, Fratzl P, Ceré S. Improving the osteointegration and bone–implant interface by incorporation of bioactive particles in sol–gel coatings of stainless steel. Acta Biomaterialia 2010;6(4):1601-1609.
7. Haïdopoulos M,Turgeon S, Laroche G, Mantovani D. Surface modifications of 316 stainless steel for the improvement of its interface properties with RFGD-deposited fluorocarbon coating . Surface and Coatings Technology 2005;197(2-3):278-287.
8. Zuo Y,Wang H, Zhao J, Xiong J. The effects of some anions on metastable pitting of 316L stainless steel. Corrosion Science 2002;44(1):13-24.
9. Hiromoto S, K. Noda, Hanawa T. Electrochemical properties of an interface between titanium and fibroblasts L929. Electrochimica Acta 2002;48(4):387-396.
10. Fadl-Allah SA, El-Sherief RA, Badawy WA. Electrochemical formation and characterization of porous titania (TiO2) films on Ti. J Appl Electrochem 2008;38:1459–1466.
11. Fadl-Allah SA, Mohsen Q. Characterization of native and anodic oxide films formed on commercial pure titanium using electrochemical properties and morphology techniques. Applied Surface Science 2010;256:5849-5855.
12. Cabrini RL, Guglielmotti MB, Almagro JC. Histomorphometry of initial bone healing around
zirconium implants in rats. Implant Dent 1993;2**:**264–67.
13. Ohkawa H, Ohishi N, Yagi K. Assay for lipid peroxides in animal tissues by thiobarbituric acid reaction. Analyt Biochem 1979;95:351–358.
14. Beutler E, Olga D, Kelly M. Improved method for determination of blood glutathione. From the department of medicine. J Lab Clin Med (1963);61:882-88
15. Drury RAB, Wallington EA, Carleton's histological technique (fifth ed.), Oxford University Press, Oxford, New York, Toronto. 1980.
16. Rosliza R, Senin HB, Wan Nik WB. Electrochemical properties and corrosion inhibition of AA6061 in tropical seawater. Colloids and Surfaces A:physicochem.Eng.Aspects 2008;312:185-189.
17. Khaled KF, Fadl-Allah SA, Hammouti B. Some benzotriazol derivatives as corrosion inhibitors for copper in acidic medium: Experimental and quantum chemical molecular dynamics approach. Materials Chemistry and Physics 2009;117:148-155.
18. Mohammed AA. Metastable and stable pitting events on Al induced by chlorate and perchlorate anions – Polarization,XPS and SEM studies 2009; 54:1857-1863.
19. Al-Mobarak NA, Al-Mayouf AM, Al-Swayih AA. The effect of hydrogen peroxide on the electrochemical behavior of Ti and some of its alloys for dental applications. Materials Chemistry and Physics 2006; 99: 333-340.
20. Chaves R, Costa I, de Melo HG, Wolynec S. Evaluation of selective corrosion in UNS S31803 duplex stainless steel with electrochemical impedance spectroscopy. Electrochim Acta 2006; 51:1842-6.
21. Elki CS, Sergio MR, Joao MDAR. Influence of chloride ion concentration and temperature on the electrochemical properties of passive films formed on a superduplex stainless steel 2010;61:240-244.
22. Marcus P, Maurice V, Strehblow HH. Localized corrosion (pitting): a model of passivity breakdown including the role of the oxide layer nanostructure. Corrosion Scicence 2008; 50:768-780.
23. Rena P-G, Lee S-W, Biswaland S, Goodman SB. Systemic trafficking of macrophages induced by bone cement particles in nude mice. Biomaterials. 2008; 29(36):4760-4765.
24. Dufuor DR, Lott JA, Nolte FS, Gretch DR, Koff RS, Seeff LB. Diagnosis and monitoring of hepatic injury. Performance characteristics of laboratory tests. Clin Chem 2000; 46:2027-2049.
25. McCuskey RS, Sipes IG. Differential hepatotoxicity induced by cadmium in Fischer 344 and Sprague–Dawley rats. Toxicol Sci 2002; 65:151–159.
26. Morals S, Pereira MC. Applied Methodology: Application of stripping voltammetry and microelectrodes *in vitro* biocompatibility and in vivo toxicity tests of AISI 316L corrosion products. J Trace Elements Med Biol 2000; 14:48–54.
27. Mattson MP. Modification of ion homeostasis by lipid peroxidation: roles in neuronal degeneration and adaptive plasticity. Trends Neurosci 1998; 21:53–57.
28. Jaeschke H, Gores GJ, Cederbaum AI, Hinson JA, Pessayre D, Lemasters JJ. Mechanisms of hepatotoxicity. Toxicol Sci 2002; 65:166-176.
29. Xia T, Kovochich M, Brant J, Hotze M, Sempf J, Oberley T, Sioutas C, Yeh JI, Wiesner MR, Nel AE. Comparison of the abilities of ambient and manufactured nanoparticles to induce cellular toxicity according to an oxidative stress paradigm. Nano. Letters. 2006; **6**(8) 1794–1807.
30. Hayes JD, Flanagan J, Jowsey U. Glutathione transferases, Annual Reviews in Pharmacol Toxicol 2005; 45:51–88.
31. Oliveira M, Santos˙ MA and Pacheco M. Glutathione protects heavy metal-induced inhibition of hepatic microsomal ethoxyresorufin *O*-deethylase activity in *Dicentrarchus labrax* L. Ecotoxicol Environ Saf 2004; 58(3): 379-385.
32. Hansen-Algenstaedt N, Joscheck C, Wolfram L , Schaefer C, Müller I, Böttcher A, Deuretzbacher G, Wiesner L, Leunig M, Algenstaedt P, Rüther W. Sequential changes in vessel formation and micro-vascular function during bone repair. Acta Orthopaedica 2006; 77(3): 429-439.

11/26/2010